RESEARCH ARTICLE

Figures and figure supplements

Multiscale analysis of single and double maternal-zygotic *Myh9* and *Myh10* mutants during mouse preimplantation development

Markus Frederik Schliffka *et al*

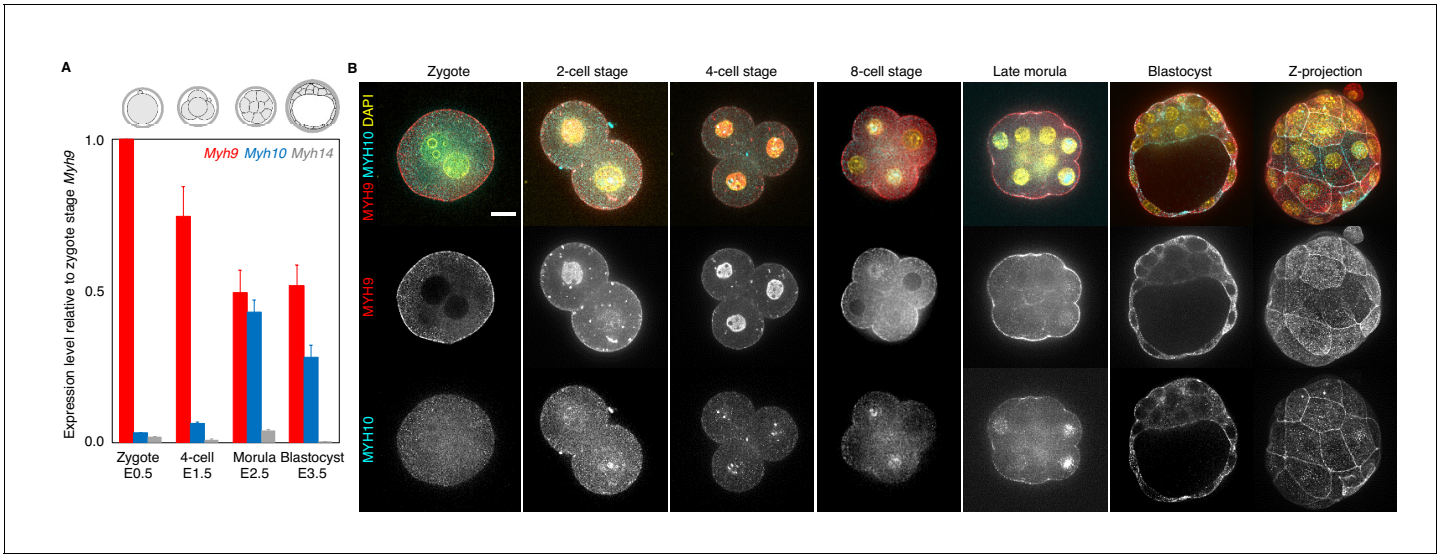

Figure 1. Expression of non-muscle myosin II heavy chain (NMHC) paralogs during preimplantation development. (**A**) RT-qPCR of *Myh9* (red), *Myh10* (blue), and *Myh14* (grey) at the zygote (E0.5, n = 234), four-cell (E1.5, n = 159), morula (E2.5, n = 189), and blastocyst (E3.5, n = 152) stages from six independent experiments. Gene expression is normalized to *Gapdh* and shown as the mean ± SEM fold change relative to *Myh9* at the zygote stage. (**B**) Representative images of immunostaining of NMHC paralogs MYH9 (red) and MYH10 (cyan) throughout preimplantation development. DAPI in yellow. Scale bar, 20 μm.

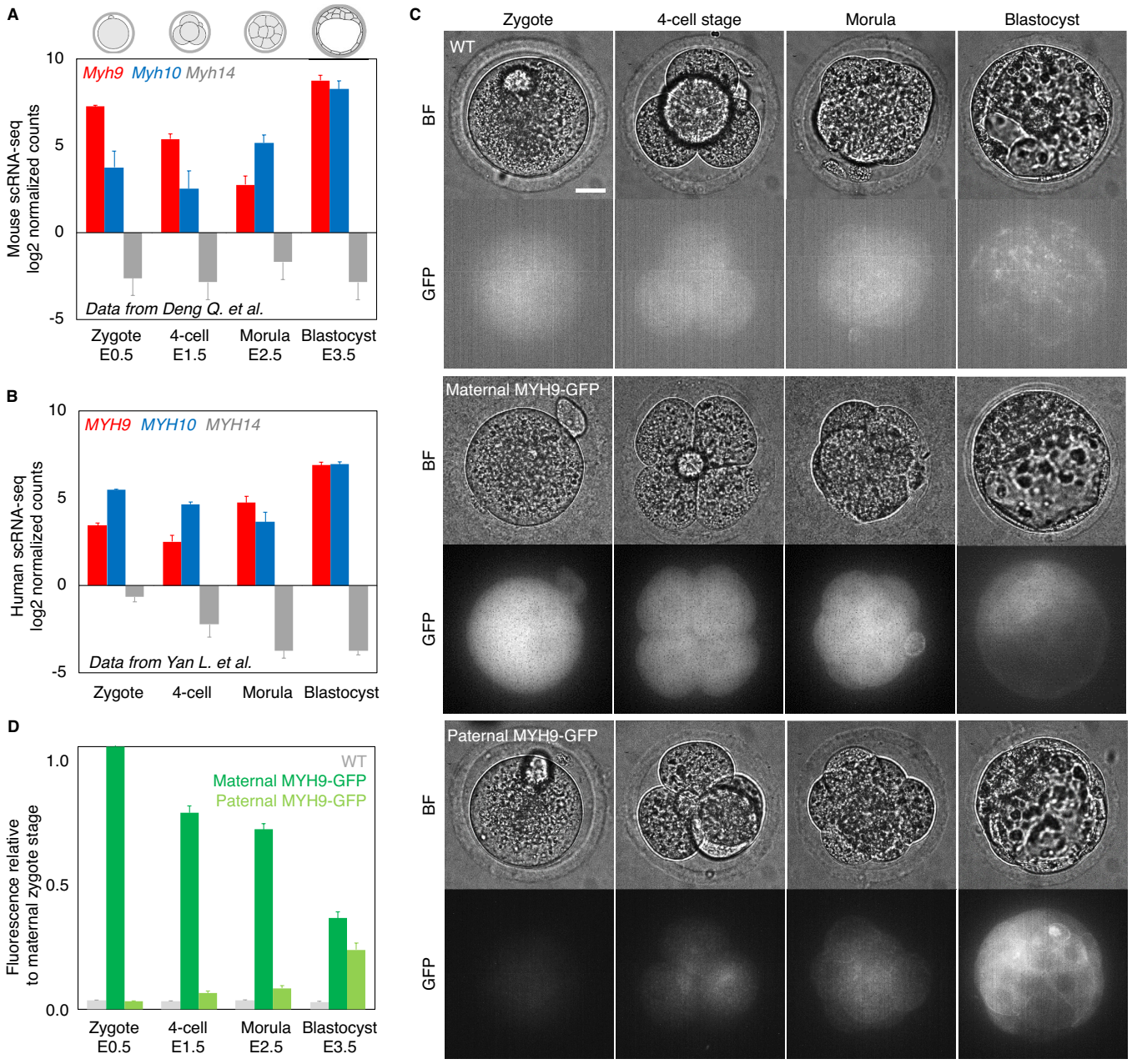

Figure 1—figure supplement 1. Analysis of the expression of non-muscle myosin II heavy chain (NMHC) paralogs during preimplantation development based on single cell RNA sequencing and MYH9-GFP fluorescence. (**A**) Mouse single cell RNA sequencing analysis adapted from ***Deng et al., 2014***, showing the expression levels of *Myh9* (red), *Myh10* (blue), and *Myh14* (grey) at the zygote, four-cell, morula, and blastocyst stages. Data show mean ± SEM. (**B**) Human single cell RNA sequencing analysis adapted from ***Yan et al., 2013***, showing the expression levels of *MYH9* (red), *MYH10* (blue), and *MYH14* (grey) at the zygote, four-cell, morula, and blastocyst stages. Data show mean ± SEM. (**C**) Representative images of WT (top) and transgenic embryos expressing a GFP-tagged version of MYH9 from their maternal (middle) or paternal (bottom) allele at the zygote, four-cell, morula, and blastocyst stages. LUT is adjusted to the brightest signal of each respective genotype. (**D**) MYH9-GFP fluorescent level normalized to maternal MYH9-GFP at the zygote stage. Data originate from three independent experiments for the WT (grey) from zygote to blastocyst stage (n = 6), maternal MYH9-GFP (dark green) zygote stage (n = 23), maternal MYH9-GFP from 4-cell stage to blastocyst stage (n = 24), and paternal MYH9-GFP (light green) from zygote to blastocyst stage (n = 22). Data show mean ± SEM. Scale bars, 20 μm.

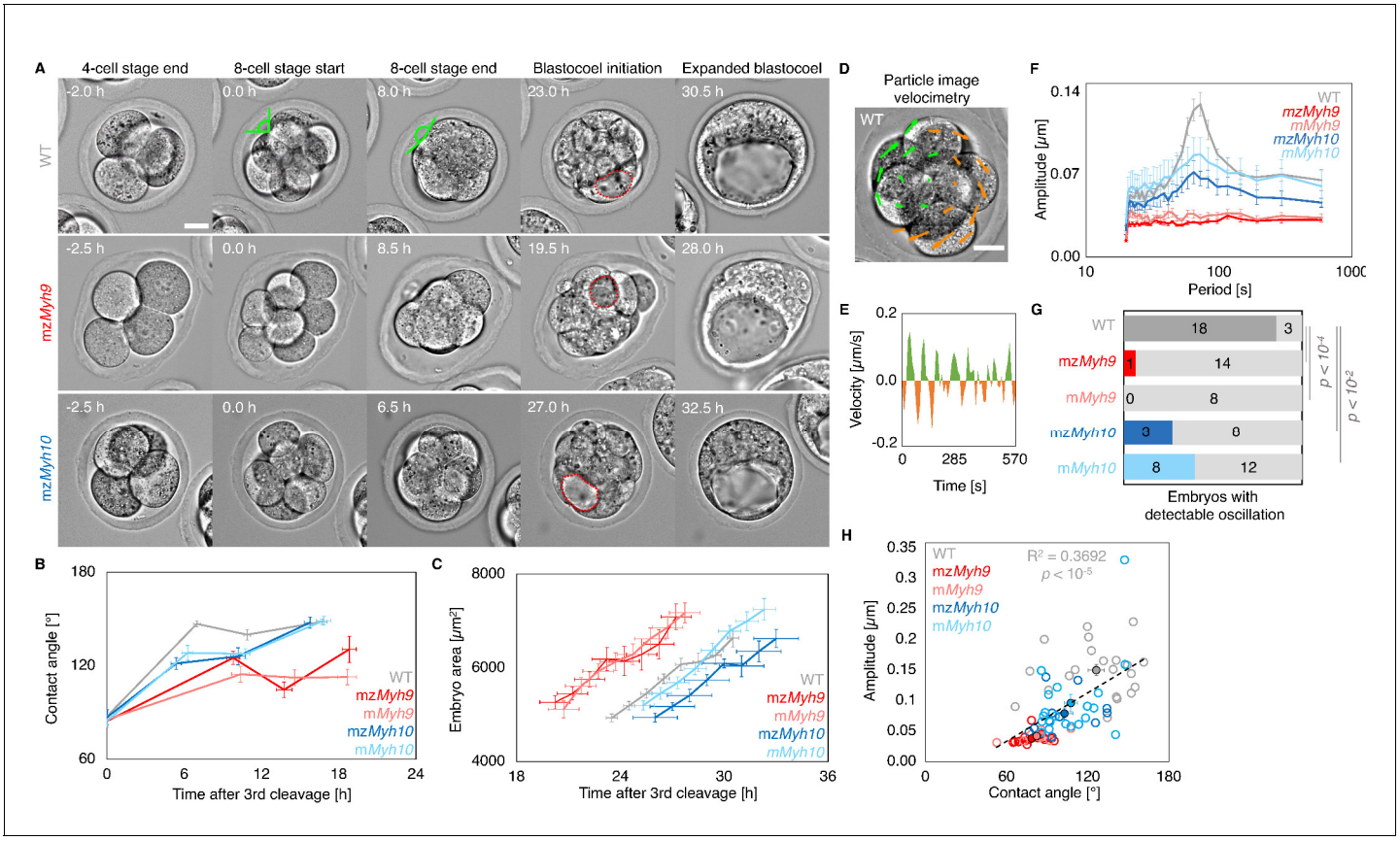

Figure 2. Multiscale analysis of morphogenesis in single maternal-zygotic *Myh9* or *Myh10* mutant embryos. (**A**) Representative images of long-term time-lapse of WT, mz*Myh9,* and mz*Myh10* embryos at the end of the 4-cell stage, start and end of the 8-cell stage, at the initiation of blastocoel formation and early blastocyst stage (see also ***Figure 2—video 1***). Scale bar, 20 µm. Time in hours after the third cleavage. Green lines mark the contact angles increasing during compaction. Dotted red lines indicate the nascent lumen. (**B**) Contact angle of WT (grey, n = 23, 23, 21, 22), mz*Myh9* (red, n = 15, 15, 10, 8), m*Myh9* (light red, n = 8, 8, 8, 3), mz*Myh10* (blue, n = 11, 11, 11, 11), and m*Myh10* (light blue, n = 20, 20, 20, 20) embryos after the third cleavage, before and after the fourth cleavage and before the fifth cleavage. Data show mean ± SEM. Statistical analyses are provided in ***Appendix 1—table 1–2***. (**C**) Embryo growth during lumen formation of WT (grey, n = 20), mz*Myh9* (red, n = 9), m*Myh9* (light red, n = 7), mz*Myh10* (blue, n = 7), and m*Myh10* (light blue, n = 13) embryos measured for seven continuous hours after a lumen of at least 20 µm in diameter is observed. Data show mean ± SEM. (**D**) Representative image of a short-term time-lapse overlaid with a subset of velocity vectors from Particle Image Velocimetry (PIV) analysis. Green for positive and orange for negative Y-directed movement. (**E**) Velocity over time for a representative velocity vector of embryo shown in D and ***Figure 2—video 2***. (**F**) Power spectrum resulting from Fourier transform of PIV analysis of WT (grey, n = 21), mz*Myh9* (red, n = 15), m*Myh9* (light red, n = 8), mz*Myh10* (blue, n = 11), and m*Myh10* (light blue, n = 20) embryos. Data show mean ± SEM. (**G**) Proportion of WT (grey, n = 21), mz*Myh9* (red, n = 15), m*Myh9* (light red, n = 8), mz*Myh10* (blue, n = 11), and m*Myh10* (light blue, n = 20) embryos showing detectable oscillations in their power spectrum (see 'Materials and methods'). Chi^2 p value comparing to WT is indicated. (**H**) Amplitude of oscillation as a function of the mean contact angle for WT (grey, n = 21), mz*Myh9* (red, n = 15), m*Myh9* (light red, n = 8), mz*Myh10* (blue, n = 11), and m*Myh10* (light blue, n = 20) embryos. Open circles show individual embryos and filled circles give mean ± SEM of a given genotype. Pearson's R^2 and p value are indicated. Statistical analyses are provided in ***Appendix 1—table 3***.

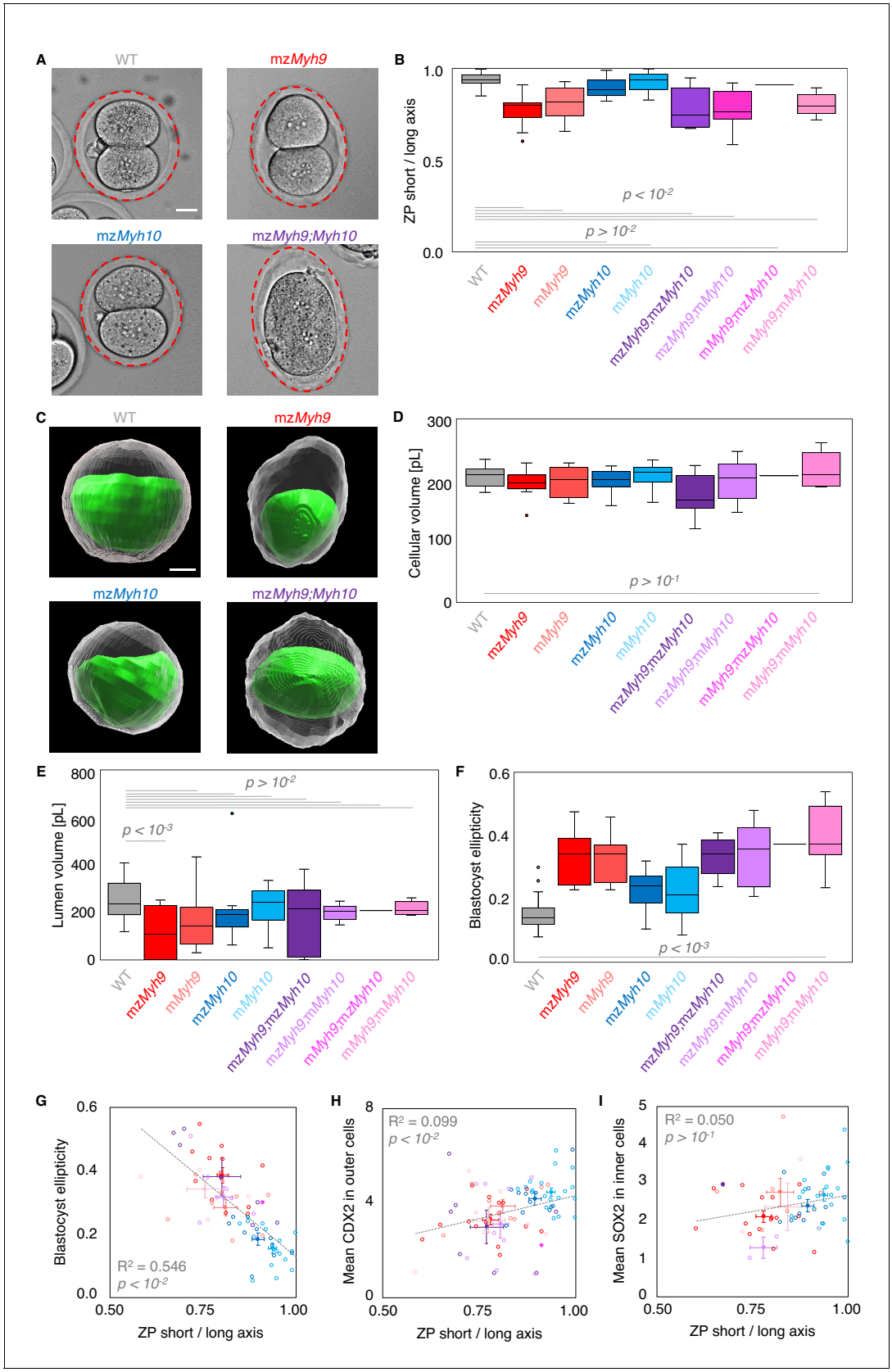

Figure 2—figure supplement 1. Macroscopic shape analysis of maternal-zygotic *Myh9* and *Myh10* mutant embryos. (**A**) Representative images of E1.5 WT, mz*Myh9*, mz*Myh10*, and mz*Myh9*;mz*Myh10* embryos. The zona pellucida is highlighted with a red ellipse. (**B**) Boxplot of the short/long axis ratio of

Figure 2—figure supplement 1 continued on next page

Figure 2—figure supplement 1 continued

an ellipse manually fitted onto the zona pellucida of E1.5 embryos that are WT (grey, n = 23), mz*Myh9* (red, n = 15), m*Myh9* (light red, n = 8), mz*Myh10* (blue, n = 11), m*Myh10* (light blue, n = 19), mz*Myh9;*mz*Myh10* (purple, n = 8), mz*Myh9;*m*Myh10* (lilac, n = 9), m*Myh9;*mz*Myh10* (pink, n = 1), and m*Myh9;* m*Myh10* (bubblegum, n = 7) mutants. (**C**) Representative images of segmented WT, mz*Myh9*, mz*Myh10*, and mz*Myh9;*mz*Myh10* blastocysts. The segmented lumen is shown in green. The cellular volume, shown in grey, results from subtracting the lumen volume from the segmented embryo volume. (**D-F**) Cellular (**D**) and lumen (**E**) volumes, and 3D oblate ellipticity (**F**) of segmented WT (grey, n = 23), mz*Myh9* (red, n = 13), m*Myh9* (light red, n = 8), mz*Myh10* (blue, n = 10), m*Myh10* (light blue, n = 16), mz*Myh9;*mz*Myh10* (purple, n = 6), mz*Myh9;*m*Myh10* (lilac, n = 8), m*Myh9;*mz*Myh10* (pink, n = 1), and m*Myh9;*m*Myh10* (bubblegum, n = 5) mutants. (**G-I**) Blastocyst ellipticity (**G**), CDX2 N/C ratio in outer cells (**H**), or SOX2 N/C ratio in inner cells (**I**) as a function of the ZP short/long axis at the 2-cell stage. mz*Myh9* (red, n = 13/15/15), m*Myh9* (light red, n = 8/8/7), mz*Myh10* (blue, n = 10/11/11), m*Myh10* (light blue, n = 16/19/19), mz*Myh9;*mz*Myh10* (purple, n = 6/7/1), mz*Myh9;*m*Myh10* (lilac, n = 8/9/2), m*Myh9;*mz*Myh10* (pink, n = 1/1/0), and m*Myh9;*m*Myh10* (bubblegum, n = 5/7/3) mutants. Open circles show individual embryos and filled circles give mean ± SEM of a given genotype. Pearson's R^2 and p value are indicated. Scale bars, 20 μm. Welch's *t* test p values compared to WT are shown.

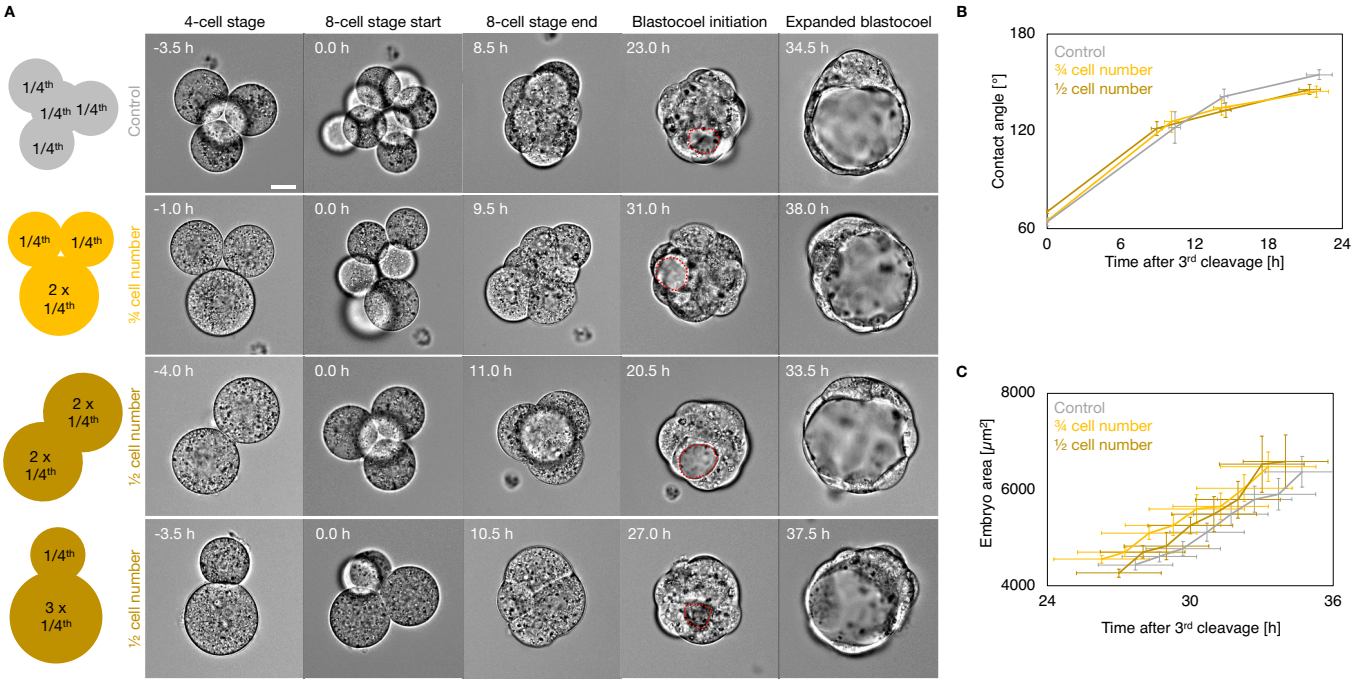

Figure 2—figure supplement 2. Morphogenesis of embryos with blastomeres fused at the 4-cell stage. (**A**) Schematic diagram of 4-cell stage embryos with four cells (control) or after fusion with three cells, two cells of equal or unequal sizes. Representative images of long-term time-lapse of embryos withfour cells (control), or after fusion with three cells, two cells of equal or unequal sizes at the end of the 4-cell stage, start and end of the 8-cell stage, at the initiation of blastocoel formation, and early blastocyst stage (***Figure 2—video 4***). Scale bar, 20 µm. Time in hours after the third cleavage. Dotted red lines indicate the nascent lumen. (**B**) Contact angle of control (grey, n = 12, 12, 12, 12), ¾ cell number (yellow, n = 12, 12, 12, 9), and ½ cell number (brown, n = 4, 4, 4, 4) embryos after the third cleavage, before and after the fourth cleavage, and before the fifth cleavage. Data show mean ± SEM. (**C**) Embryo growth during lumen formation for control (grey, n = 10), ¾ cell number (yellow, n = 11), and ½ cell number (brown, n = 4) embryos measured for seven continuous hours after a lumen of at least 20 µm is observed (as in blastocoel initiation of panel A). Data show mean ± SEM.

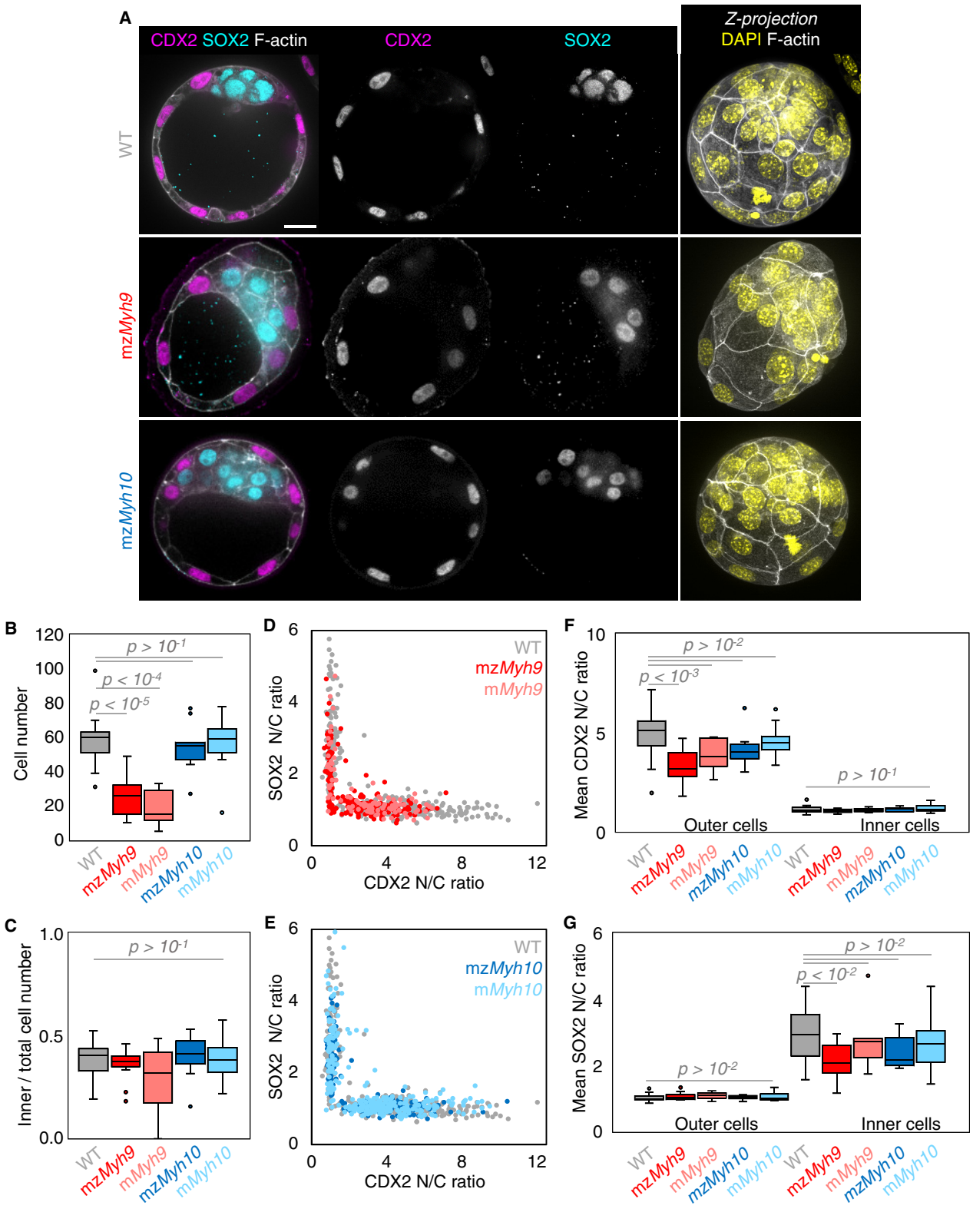

Figure 3. Analysis of TE and ICM lineages in single maternal-zygotic *Myh9* or *Myh10* mutant embryos. (**A**) Representative images of WT, mz*Myh9*, and mz*Myh10* embryos stained for TE and ICM markers CDX2 (magenta) and SOX2 (cyan), DAPI (yellow), and F-actin (grey). The same mutant embryos as in

Figure 3 continued on next page

Figure 3 continued

Figure 2A are shown. Scale bar, 20 μm. (**B-C**) Total cell number (**B**) and proportion of inner cells (**C**) in WT (grey, n = 23), mz*Myh9* (red, n = 15), m*Myh9* (light red, n = 8), mz*Myh10* (blue, n = 11), and m*Myh10* (light blue, n = 19) embryos. (**D-E**) Nuclear to cytoplasmic (N/C) ratio of CDX2 and SOX2 staining for individual cells from WT (grey, n = 345), mz*Myh9* (red, n = 204), m*Myh9* (light red, n = 95), mz*Myh10* (blue, n = 160), and m*Myh10* (light blue, n = 300) embryos. (**F-G**) Average N/C ratio of CDX2 (**F**) and SOX2 (**G**) staining for outer (left) or inner (right) cells from WT (grey, n = 23), mz*Myh9* (red, n = 15), m*Myh9* (light red, n = 8), mz*Myh10* (blue, n = 11), and m*Myh10* (light blue, n = 19) embryos. Mann-Whitney *U* test p values compared to WT are indicated.

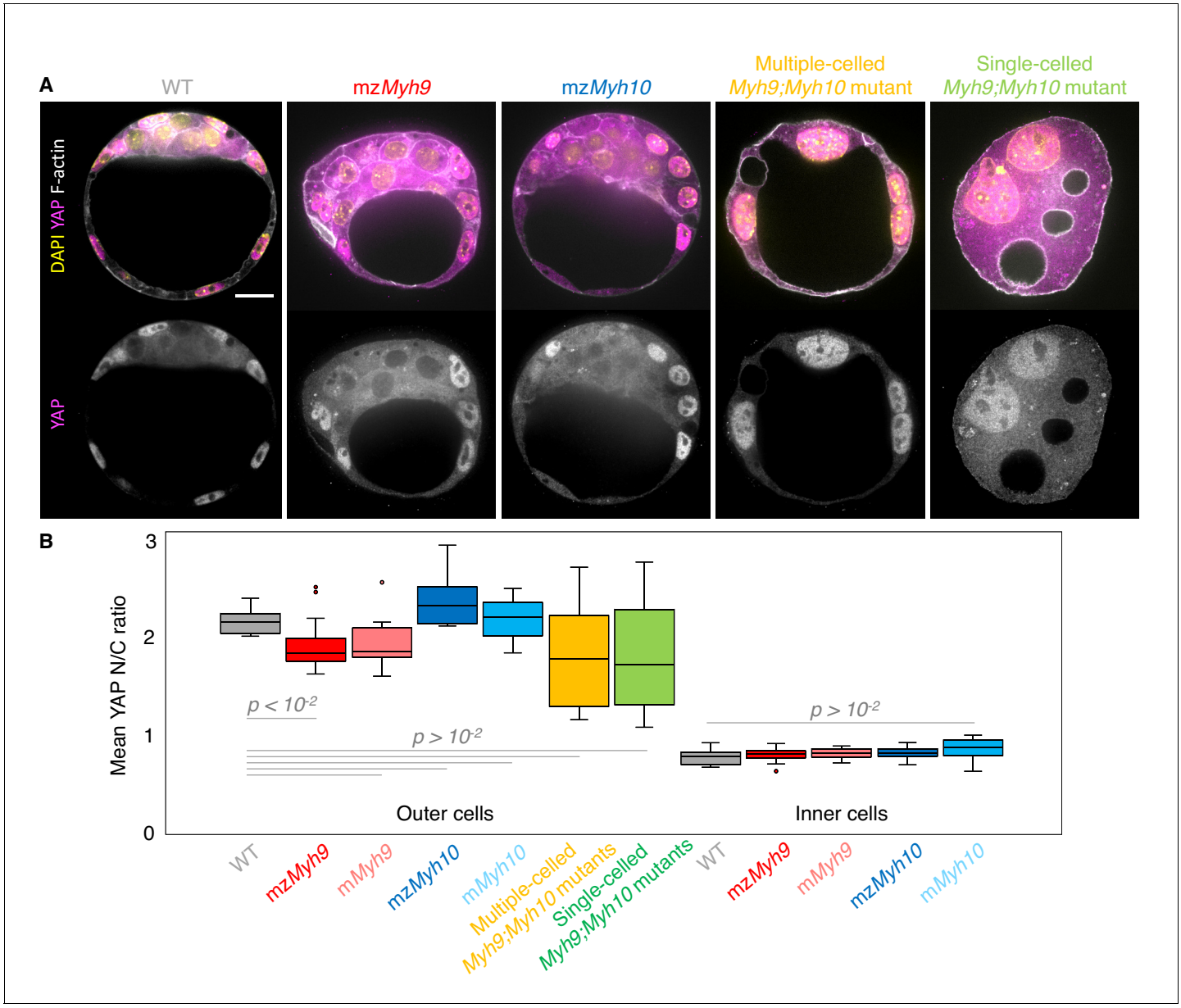

Figure 3—figure supplement 1. Analysis of YAP localization in maternal-zygotic *Myh9* and *Myh10* mutant embryos. (**A**) Representative images of WT, mz*Myh9*, mz*Myh10*, and multiple- or single-celled *Myh9;Myh10* mutant embryos stained for YAP (magenta), DAPI (yellow), and F-actin (grey). Scale bar, 20 µm. (**B**) Mean nuclear to cytoplasmic (N/C) ratio of YAP for outer and inner cells from WT (grey, n = 15), mz*Myh9* (red, n = 19), m*Myh9* (light red, n = 9), mz*Myh10* (blue, n = 6), m*Myh10* (light blue, n = 13) embryos and outer cells from multiple-celled *Myh9;Myh10* (yellow, n = 10) and single-celled *Myh9;Myh10* (green, n = 9) mutant embryos. Mann-Whitney *U* test p values compared to WT are indicated.

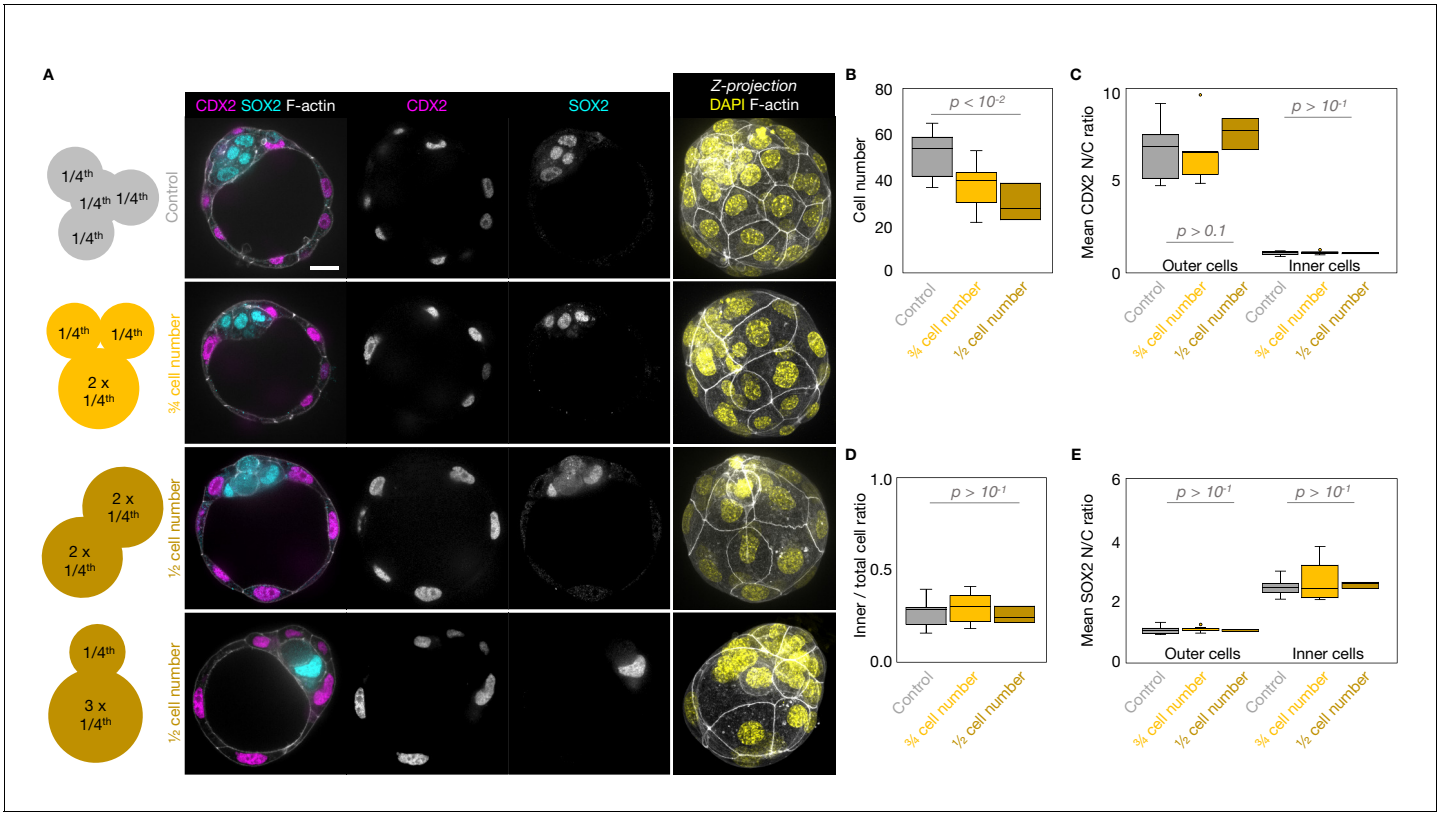

Figure 3—figure supplement 2. Lineage specification of embryos with blastomeres fused at the 4-cell stage. (**A**) Schematic diagram of 4-cell stage embryos with four cells (control) or after fusion with three cells, two cells of equal or unequal sizes. Representative images of embryos with four cells (control), or after fusion with three cells, two cells of equal or unequal sizes stained for TE and ICM markers CDX2 (magenta) and SOX2 (cyan). DAPI in yellow and F-actin in grey. The same fused embryos as in ***Figure 2—figure supplement 2A*** are shown. (**B-D**) Total cell number (**B**) and proportion of inner cells (**D**) in control (grey, n = 11), ¾ cell number (yellow, n = 9), and ½ cell number (brown, n = 3) embryos. (**C-E**) N/C ratio of CDX2 (**C**) and SOX2 (**E**) staining for outer (left) or inner (right) cells from control (grey, n = 11), ¾ cell number (yellow, n = 9), and ½ cell number (brown, n = 3) embryos. Scale bars, 20 µm. Mann-Whitney *U* test p values compared to WT are indicated.

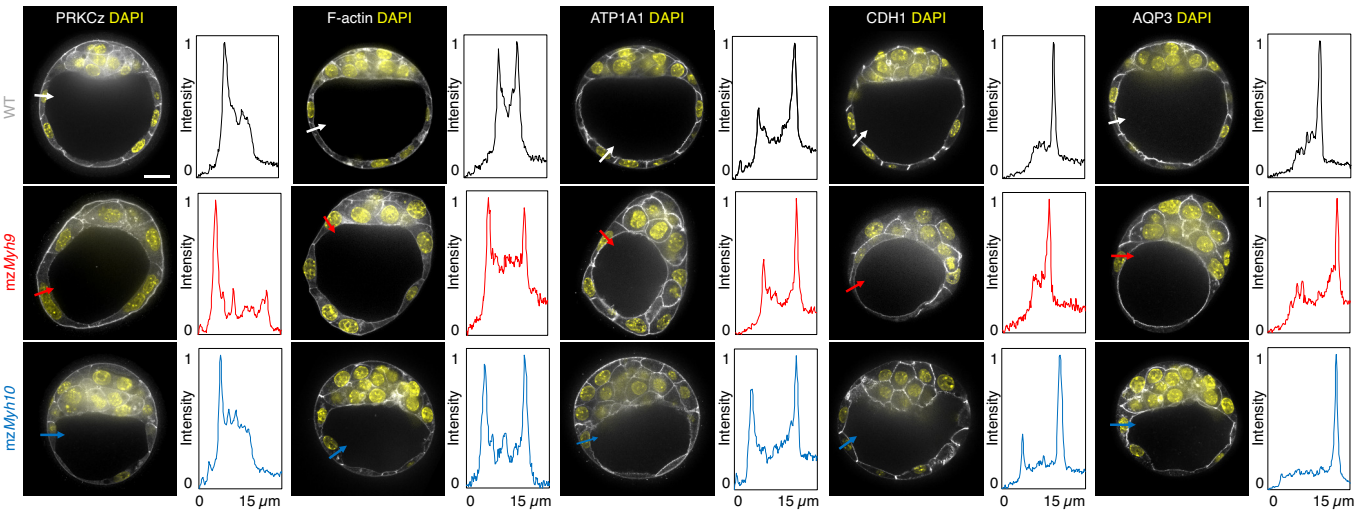

Figure 4. Apico-basal polarity of single maternal-zygotic *Myh9* or *Myh10* mutant embryos. Representative images of WT, mz*Myh9*, *and* mz*Myh10* embryos stained for apico-basal polarity markers. From left to right: PRKCz, F-actin, ATP1A1, CDH1, and AQP3 shown in grey. Nuclei stained with DAPI are shown in yellow. Intensity profiles of a representative 15 µm line drawn from the embryo surface towards the interior are shown next to each marker and genotype (arrows). Intensities are normalized to each minimal and maximal signals. Scale bar, 20 µm.

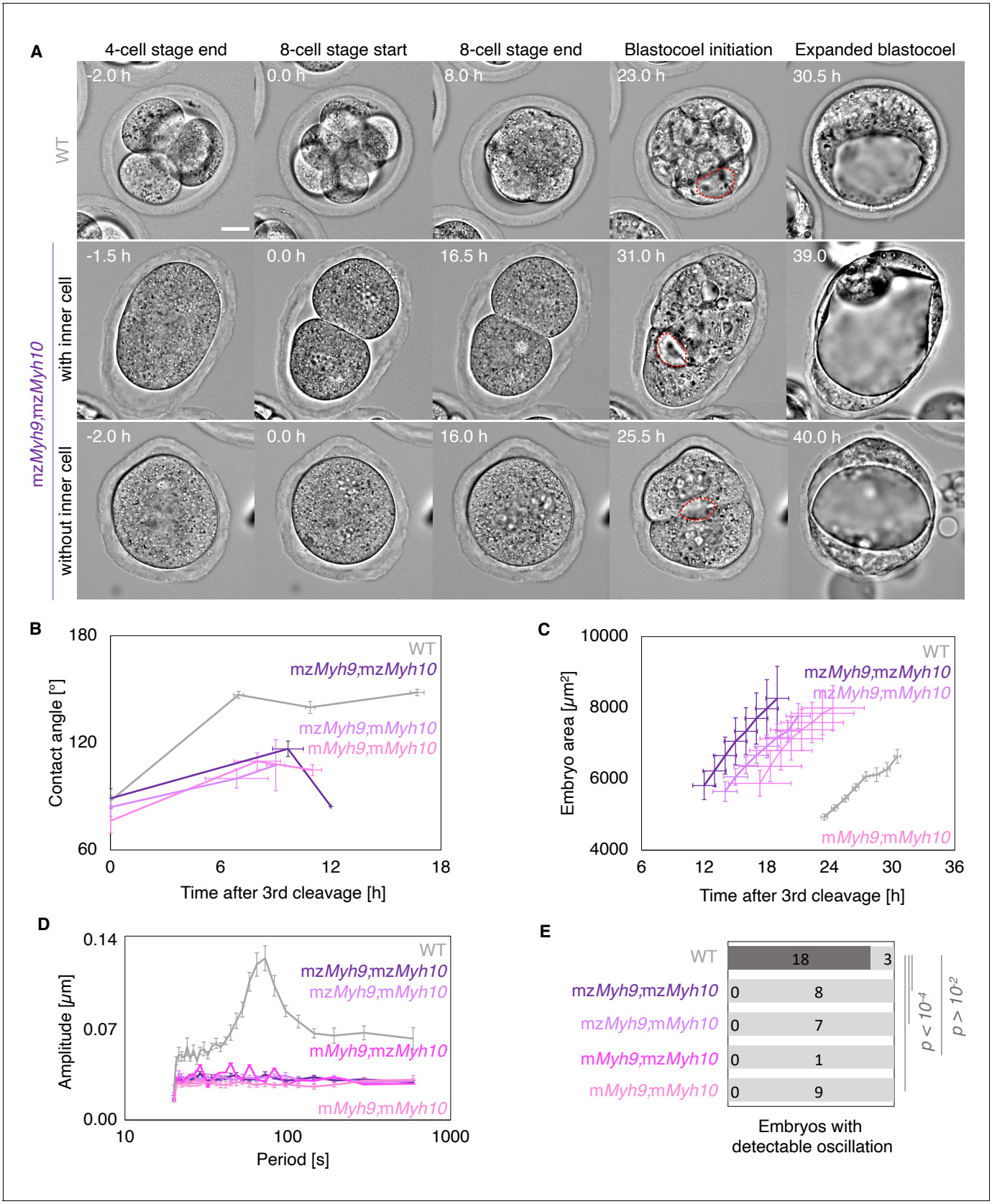

Figure 5. Multiscale analysis of morphogenesis in double maternal-zygotic *Myh9* and *Myh10* mutant embryos. (**A**) Representative images of long-term time-lapse of WT and mz*Myh9*;mz*Myh10* embryos at the end of the 4-cell stage, start and end of the 8-cell stage, at the initiation of blastocoel

Figure 5 continued on next page

Figure 5 continued

formation, and early blastocyst stage (***Figure 5—video 1***). The middle row shows an embryo that cleaved once at the time of the third cleavage and twice at the time of the fourth cleavage, which produces an embryo with one inner cell. The bottom row shows an embryo that cleaved once at the time of the fourth cleavage, which produces an embryo without inner cell. Scale bar, 20 μm. (**B**) Contact angle of WT (grey, n = 23, 23, 21, 22), mz*Myh9;* mz*Myh10* (purple, n = 7, 3, 1), mz*Myh9;*m*Myh10* (lilac, n = 7, 4, 2), and m*Myh9;*m*Myh10* (bubblegum, n = 7, 5, 3) embryos after the third cleavage, before and after the fourth cleavage, and before the fifth cleavage, when available. Data show mean ± SEM. Statistical analyses are provided in ***Appendix 1—table 1–2***. (**C**) Embryo growth during lumen formation for WT (grey, n = 20), mz*Myh9;*mz*Myh10* (purple, n = 5), mz*Myh9;*m*Myh10* (lilac, n = 6), and m*Myh9;*m*Myh10* (bubblegum, n = 6) embryos measured for seven continuous hours after a lumen of at least 20 μm is observed. Data show mean ± SEM. (**D**) Power spectrum resulting from Fourier transform of PIV analysis of WT (grey, n = 21), mz*Myh9;*mz*Myh10* (purple, n = 8), mz*Myh9;* m*Myh10* (lilac, n = 7), m*Myh9;*mz*Myh10* (pink, n = 1), and m*Myh9;*m*Myh10* (bubblegum, n = 9) embryos. Data show mean ± SEM. (**E**) Proportion of WT (grey, n = 21), mz*Myh9;*mz*Myh10* (purple, n = 8), mz*Myh9;*m*Myh10* (lilac, n = 7), m*Myh9;*mz*Myh10* (pink, n = 1), and m*Myh9;*m*Myh10* (bubblegum, n = 9) embryos showing detectable oscillations in their power spectrum. Chi^2 test p value compared to WT is indicated.

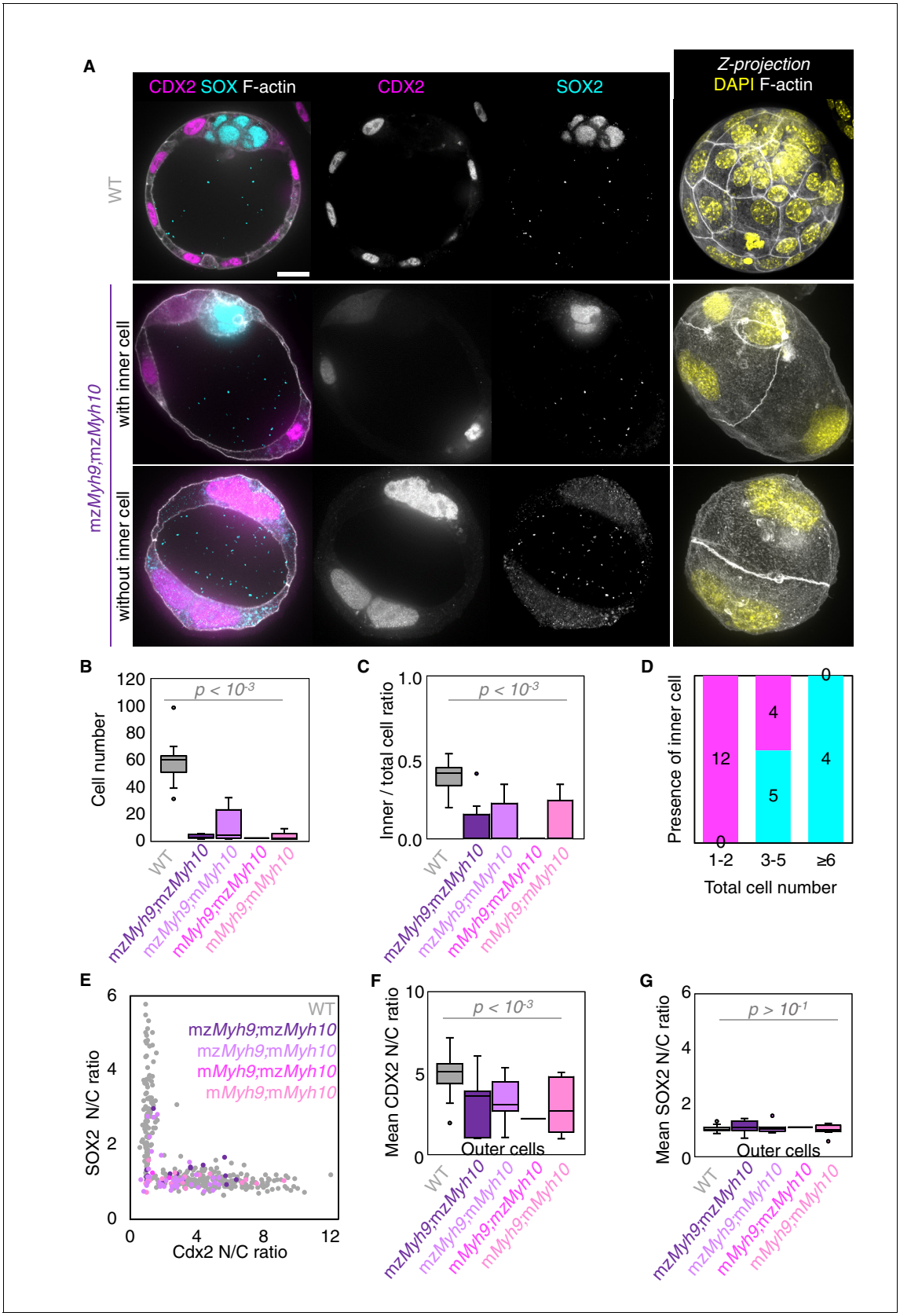

Figure 6. Analysis of TE and ICM lineage in double maternal-zygotic *Myh9* and *Myh10* mutant embryos. (**A**) Representative images of WT and mz*Myh9;* mz*Myh10* embryos stained for TE and ICM markers CDX2 (magenta) and SOX2 (cyan), DAPI (yellow), and F-actin (grey). The same mutant embryos as in

Figure 6 continued on next page

Figure 6 continued

Figure 5A are shown. Scale bar, 20 μm. (**B-C**) Total cell number (**B**) and proportion of inner cells (**C**) in WT (grey, n = 23), mz*Myh9;*mz*Myh10* (purple, n = 8), mz*Myh9;*m*Myh10* (lilac, n = 7), m*Myh9;*mz*Myh10* (pink, n = 1), and m*Myh9;*m*Myh10* (bubblegum, n = 9) embryos. (**D**) Number of maternal *Myh9; Myh10* mutant embryos with (cyan) or without (magenta) inner cells as a function of the total number of cells. (**E**) Nuclear to cytoplasmic (N/C) ratio of CDX2 and SOX2 staining for individual cells from WT (grey, n = 345), mz*Myh9;*mz*Myh10* (purple, n = 17), mz*Myh9;*m*Myh10* (lilac, n = 41), m*Myh9;* mz*Myh10* (pink, n = 2), and m*Myh9;*m*Myh10* (bubblegum, n = 21) embryos. (**F-G**) N/C ratio of CDX2 (**F**) and SOX2 (**G**) staining for outer cells from averaged WT (grey, n = 23), mz*Myh9;*mz*Myh10* (purple, n = 8), mz*Myh9;*m*Myh10* (lilac, n = 7), m*Myh9;*mz*Myh10* (pink, n = 1), and m*Myh9;*m*Myh10* (bubblegum, n = 9) embryos. Mann-Whitney *U* test p values compared to WT are indicated.

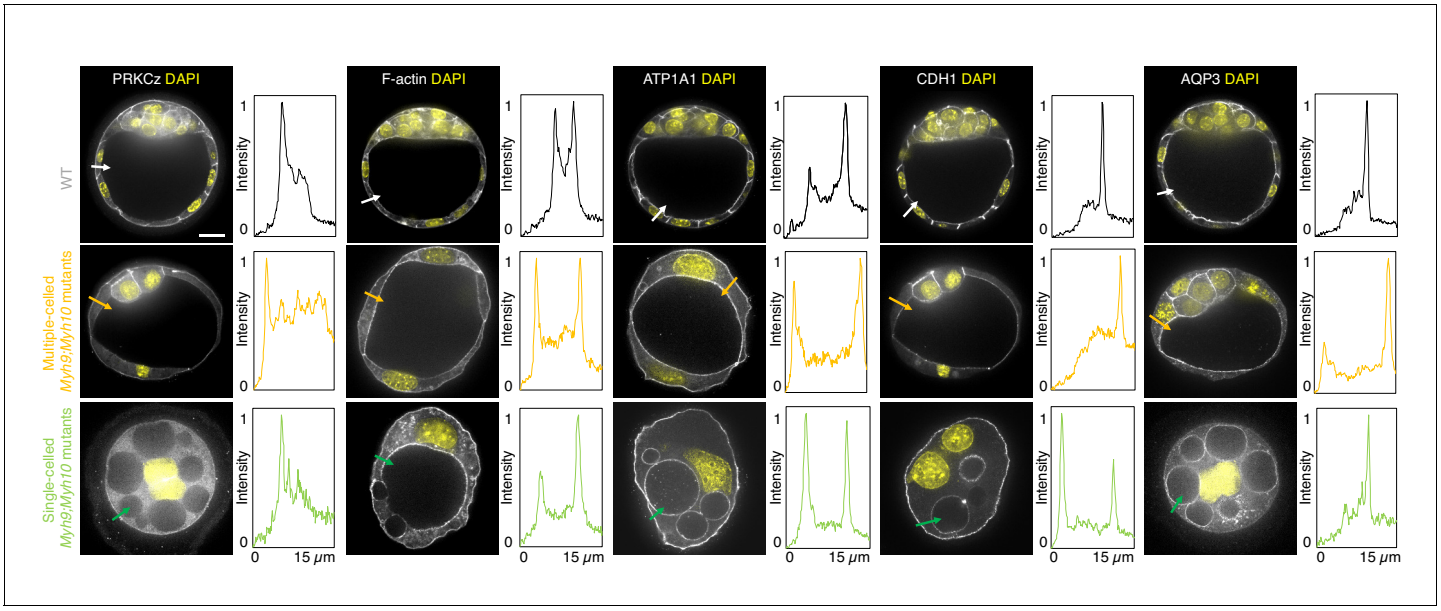

Figure 7. Apico-basal polarity of maternal *Myh9;Myh10* mutant embryos composed of multiple cells or a single cell. Representative images of WT, multiple- or single-celled *Myh9;Myh10* mutant embryos stained for apico-basal polarity markers. From left to right: PRKCz, F-actin, ATP1A1, CDH1, and AQP3 shown in grey. Nuclei stained with DAPI shown in yellow. Intensity profiles of a representative 15 μm line drawn from the embryo surface towards the interior are shown next to each marker and genotype (arrows). Intensities are normalized to each minimal and maximal signals. Scale bar, 20 μm.

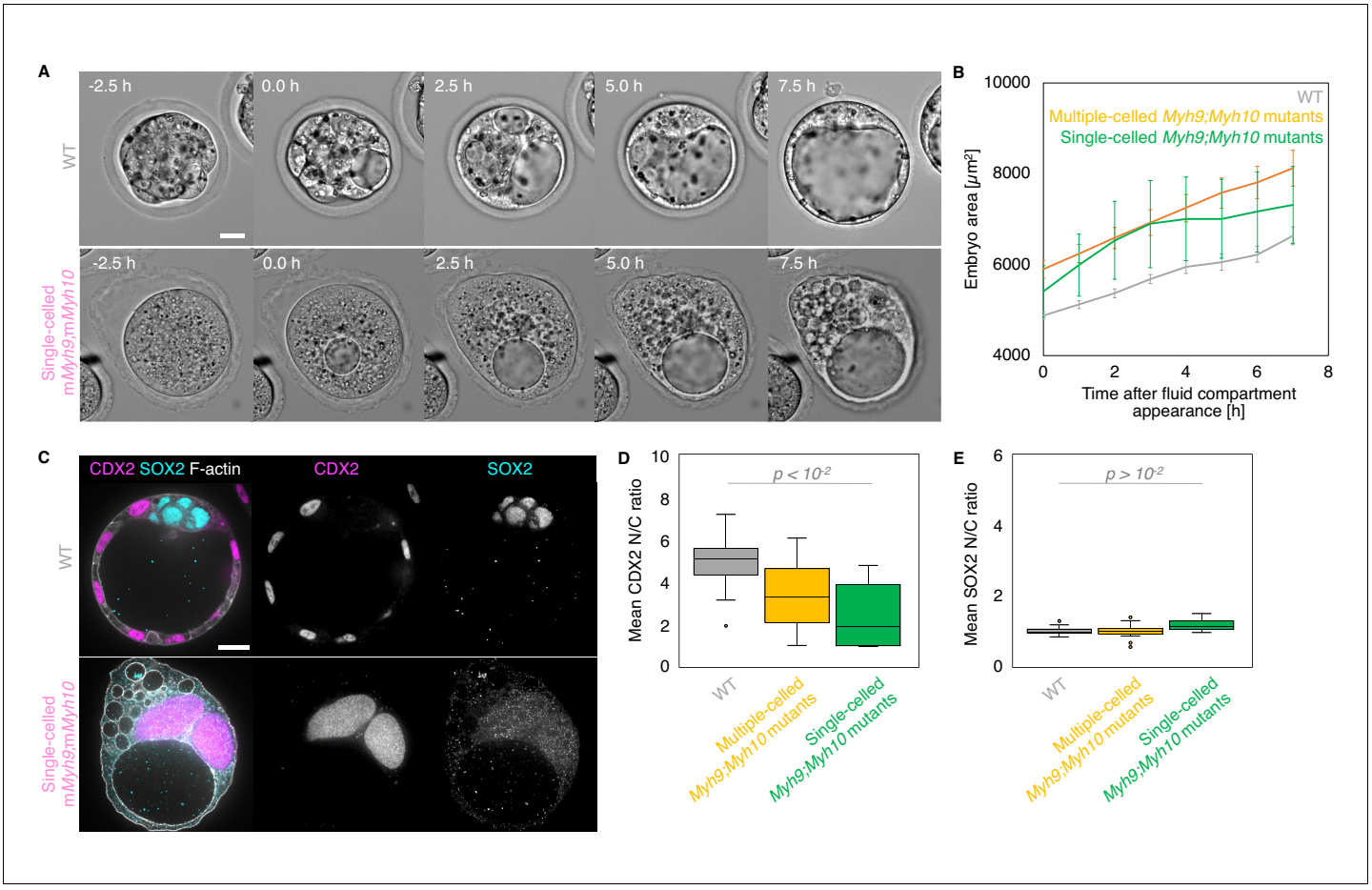

Figure 8. Single-celled embryos at the blastocyst stage. (**A**) Representative images of long-term time-lapse of WT and single-celled m*Myh9;*m*Myh10* embryos at the onset of fluid accumulation (***Figure 8—video 1***). Scale bar, 20 µm. (**B**) Embryo growth curves during fluid accumulation for WT (grey, n = 20) and multiple- (yellow, n = 13) or single-celled *Myh9;Myh10* (green, n = 4) mutant embryos measured for seven continuous hours after a lumen of at least 20 µm is observed. Data show mean ± SEM. (**C**) Representative images of WT and single-celled m*Myh9;*m*Myh10* embryos stained for TE and ICM markers CDX2 (magenta) and SOX2 (cyan), DAPI (yellow), and F-actin (grey). The same mutant embryos as in A are shown. Scale bar, 20 µm. (**D-E**) N/C ratio of CDX2 (**D**) and SOX2 (**E**) staining for outer cells from WT (grey, n = 23) and multiple- (yellow, n = 18) or single-celled *Myh9;Myh10* (green, n = 6) embryos. Mann-Whitney *U* test p values compared to WT are indicated.

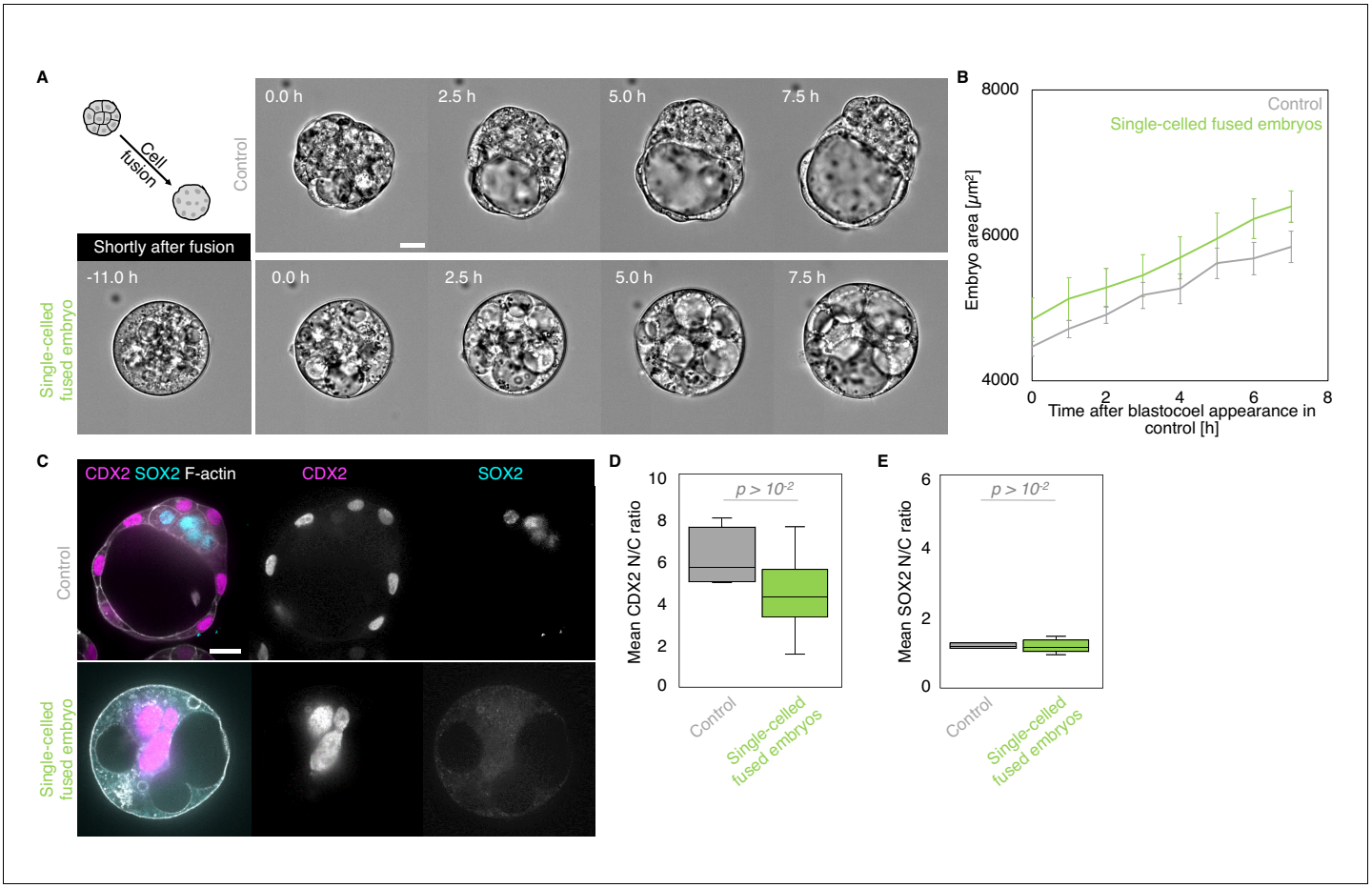

Figure 8—figure supplement 1. Morphogenesis and lineage specification of embryos with all blastomeres fused at the late morula stage. (**A**) Representative images of long-term time-lapse of control and fused single-celled embryos at the onset of fluid accumulation (***Figure 8—video 2***). A schematic diagram of the cell fusion process is shown, with a picture of the representative fused embryo shown right after the fusion. Scale bar, 20 µm. (**B**) Embryo growth curves during fluid accumulation for control (grey, n = 8) and fused single-celled (light green, n = 7) embryos measured for seven continuous hours after a lumen of at least 20 µm is observed. Data show mean ± SEM. (**C**) Representative images of control and fused single-celled embryos stained for TE and ICM markers CDX2 (magenta) and SOX2 (cyan), DAPI (yellow), and F-actin (grey). Scale bar, 20 µm. (**D-E**) N/C ratio of CDX2 (**D**) and SOX2 (**E**) staining for outer cells from averaged control (grey, n = 4) and fused single-celled (light green, n = 6) embryos. Mann-Whitney *U* test p values compared to control are indicated.